Analyst

Accepted Manuscript

This article can be cited before page numbers have been issued, to do this please use: Y. Zhang, F. Yang, Z. Sun, Y. Li and G. Zhang, *Analyst*, 2017, DOI: 10.1039/C7AN00988G.

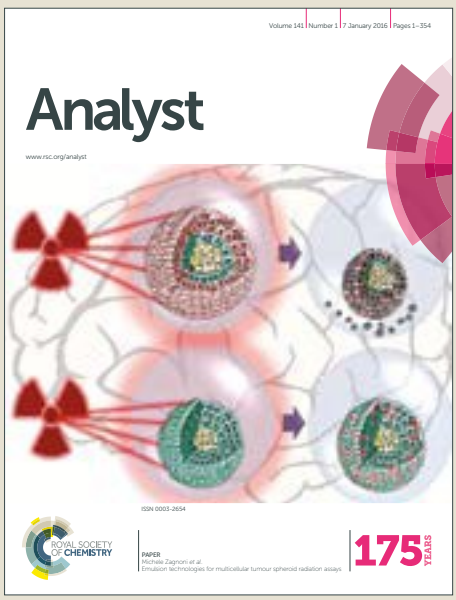

ROYAL SOCIETY OF CHEMISTRY

rsc.li/analyst

View Article Online
DOI: 10.1039/C7AN00988G

Surface acoustic wave biosensor synergizing DNA-mediated in-situ silver nanoparticle growth for highly specific and signal-amplified nucleic acid assay

Yulin Zhang[1], *Fan Yang*[*,1], *Zhongyue Sun*[1], *Yu-Tao Li*[1], *Guo-Jun Zhang*[*,1]

[1]School of Laboratory Medicine, Hubei University of Chinese Medicine, 1 Huangjia Lake West Road, Wuhan 430065, China.

*Corresponding author: Tel: +86-27-68890259, Fax: +86-27-68890259

E-mail: yangf2013@hbtcm.edu.cn; zhanggj@hbtcm.edu.cn

View Article Online
DOI: 10.1039/C7AN00988G

Abstract

This work reports a surface acoustic wave (SAW) DNA sensor that synergizes the surface mass effect for signal-amplified and sequence-specific DNA detection in blood serum. By combining an enzyme-mediated DNA extension reaction (both viscoelastic and mass fraction) with in-situ synthesis of silver nanoparticles (mass fraction), a highly sensitive SAW biosensing interface with synergic mass loading was tailor-engineered. As target DNA hybridized with the surface-confined capture probes, the exposed 3'-OH terminal of the target sequence could be triggered to elongate in the coexistence of terminal deoxynucleoside transferase (TdT) and deoxy-ribonucleoside triphosphate (dNTP), thereby producing an evident mass effect. Importantly, the extended domain can serve as a template to specifically hybridize with Ag^+-binding sequences. In the presence of reducing agents, the accumulated silver ions would nucleate for in-situ synthesis of silver nanoparticles, further enhancing the mass loading. By using this approach, we observed a rapid growing event of silver nanoparticles for signal enhancement, which improved the detection limit (0.8 pM) of the SAW sensor by 3 orders of magnitude as compared to the strategy without signal amplification (at nanomolar level). The sensor also achieved a high specificity in discriminating even single-mismatched DNA sequence, and meanwhile could probe the low-abundance DNA molecules directly in human serum with minimal interference. These advantages make the SAW biosensor promising for practical applications, such as monitoring of molecular interactions and disease diagnostics.

Keywords: Surface acoustic wave biosensor; DNA detection; Terminal deoxynucleoside transferase; Silver nanoparticles; Signal amplification

View Article Online
DOI: 10.1039/C7AN00988G

1. Introduction

Generally, surface acoustic wave (SAW) sensor is fabricated on a piezoelectric substrate, such asquartz and lithium tantalate ($LiTaO_3$), with interdigital transducers (IDT) that generate and detect acoustic wave signals on the sensor surface.[1, 2] Because the acoustic energy is strongly confined at the surface of SAW sensor, any physical, chemical or conductive changes close to the surface would perturb the propagating acoustic wave (*e.g.,* Love wave) and correspondingly alter the wave velocity, phase or amplitude.[1] For example, the adsorbed biomolecules often induce the changes in mass and viscosity of the sensing layer in SAW biosensor.[1] To achieve high sensitivity of biodetection, the Love wave sensor applies shear waves in an additional amorphous guiding layer, which allows the acoustic waves only to be marginally damped in an aqueous environment.[1] There are two types of output signal for SAW biosensor in general: phase signal and amplitude signal. It was reported that an additional rigid mass on the sensor surface results in a pure phase shift proportional to the mass loading, while changes in the viscosity lead to a combined phase shift and change in amplitude.[3,4] Both signal types have been incorporated into SAW sensors for the detection of molecules based on their specific interaction with the immobilized receptors on chip surface.[1] Because of several typical advantages, such as real-time and multiple readout, the SAW sensors have been broadly applied to detect a plethora of biologically relevant species ranging from antibiotics, neurotransmitters, proteins, nucleic acids to bacteria.[5-11]

Despite the progress, SAW biosensors still face challenges in direct readout of low-abundance molecules, particularly lack of an effective means to synergize the mass-viscosity effect for signal-enhanced bioassay.[1] Therefore, the strategy to extract the viscosity-induced mass-loading signals from the sensing layer is highly pursued in order to enhance the SAW response to the targets of interest. To achieve this, multiple functional materials, such as graphene oxide, molecularly imprinted polymer and single-wall carbon nanotube, have been used as sensitive layers to increase the susceptibility of SAW biosensors.[6,8,12,13]. Nevertheless, the sensitivity in most of these approaches was only improved within an order of magnitude. Although gold nanoparticles can improve the sensitivity to a large extent via deposition,[14, 15] there are still some drawbacks, for example, the requirement of multi-step labeling and purification. In this typical sandwich immunoassay, the signal fraction may be

View Article Online
DOI: 10.1039/C7AN00988G

exclusively contributed by the mass effect of antibody-particle conjugates, which ignores the viscosity portion. Indeed, a synergistic mass-viscosity effect can boost the phase signal because the morphology change, like molecular crowding or conformation switch, induced by the mass accumulation can also alter the propagation of SAW.[16] Binding with short DNA strands often influences the mass fraction of the SAW signal, whereas with elongated sequences, the viscoelastic fraction would be predominant as they behave like a purely viscous layer close to the sensor surface.[16,17] Thus, the metal nanoparticle-DNA complex, particularly for prolonged DNA, could serve as an ideal candidate to enhance the sensitivity of SAW sensor by combining the synergistic mass effect.[18]

Of note, DNA strands often act as templates for in-situ synthesis of metal nanoparticles (*e.g.,* silver nanoparticles, AgNPs) through direct reduction of the specifically bound metal ions.[19-21] For example, DNA-silver nanoclusters can form in the presence of both the cytosine-rich DNA templates and silver ions, which are stabilized by the DNA scaffolds and exhibit excellent spectral properties as fluorescent probes.[22,23] Moreover, these metal nanoclusters can function as nucleation sites for further growth of silver nanoparticles.[23,24] As compared to the extensive attention paid to their optical properties, such as fluorescence and plasmonics, the mass effect of DNA-metal nanoclusters or nanoparticles has relatively less been explored.[18,25,26] Indeed, the acoustic wave signal of another microgravimetric sensor, quartz-crystal-microbalance (QCM), can be largely improved by the catalyzed deposition of gold on DNA-linked Au-nanoparticles.[18] Note that such a high sensitivity may benefit from the synergic mass and viscosity effect. Nevertheless, such an effective signal-enhancing strategy has not been adapted to SAW biosensor for low-abundance molecules detection.

In this work, we report a surface-confined template-free DNA extension strategy that induces in-situ growth of AgNPs on SAW sensor surface to exploit the synergistic mass-viscosity effect for signal-amplified and sequence-specific detection of nucleic acids. The terminal deoxynucleoside transferase (TdT) can directly catalyze the addition of multiple dATP to the target sequence as it hybridizes with the capture probes and exposes its 3′-OH terminal.[27, 28] The elongated polyA sequence, thus, can serve as a template to bind the Ag^{+}-specific sequence with repeated thymine end. In the presence of reduced agents, the accumulated silver nanoclusters can gradually

View Article Online
DOI: 10.1039/C7AN00988G

grow into AgNPs that amplify the mass loading effect on SAW sensing surface, where the polyA endows a viscoelastic-mass effect. Such a synergic effect improves the sensitivity of the SAW biosensors by 3 orders of magnitude. Moreover, the Love-wave sensing platform is successfully applied to probe the low-abundance DNA molecules in human serum with minimal interference.

2. Experimental Section

2.1. Reagents and Samples

Table 1. Sequences of involved oligonucleotides.

Name	Sequence (5'-3')
Capture probe	TCATGACTTATCACAGTAGTAA-$(CH_2)_6$-SH
Target DNA	TTACTACTGTGATAAGTCATGA
Ag^+-specific probe	TTTTTTTTTTCCCCCCCCCCCC
Random sequence	TTTTTTTTTTAGATAGTCAGTC
Poly-T	TTTTTTTTTT
One-mismatched DNA[a]	TTACTACTGTGATA***T***GTCATGA
Two-mismatched DNA	TTACTAC***T***TGATA***T***GTCATGA
Three-mismatched DNA	TTACTAC***G***TGATA***T***GTC***T***TGA
NoncognateDNA	TACAAGCTCATACTACGATCATC

[a]The mismatched site is highlighted with italic and black underline

6-Mercapto-1-hexanol (MCH), silver nitrate ($AgNO_3$), sodium borohydride ($NaBH_4$), were purchased from Sigma-Aldrich (St. Louis, MO, USA). Both TdT and dATP were purchased from Takara Biotechnology Co. Ltd. (Dalian, China) and all DNA oligonucleotides (Table 1) were synthesized and purified using HPLC by Sangon Biotechnology Co. Ltd. (Shanghai, China). All the other reagents employed were of analytical grade and used without further purification. Human serum was obtained from Wuhan Third Hospital (Wuhan, China). The following buffer solutions were employed in this study: DNA immobilization buffer (10 mM phosphate, 15 mM TCEP, pH 7.4), hybridization buffer (10 mM phosphate, 50 mM $NaNO_3$, pH 7.4). chip washing buffer (10 mM phosphate, pH 7.4), SAW running buffer (10 mM phosphate, 50 mM $NaNO_3$, pH 6.8). The oligonucleotide stock solution was stored at

View Article Online
DOI: 10.1039/C7AN00988G

4°C before use. Ultrapure water obtained from a Millipore water purification system (18.2 MΩ cm^{-1} resistivity, Milli-Q Direct 8) was used in all runs.

2.2. Preparation of the Sensor Chip

The preparation of the detection chip was carried out as follows: 1) The chip with gold surface was cleaned by sonicating it in water and ethanol for 5 min, respectively; 2) The detection channels of the chip were immediately dropped with 20 μL of thiolated capture probes (3′-SH terminal) at appropriate concentrations and placed in the dark for 12 h at room temperature for self-assembly via Au-S bond; 3) The chip was subsequently treated with 20 μL of 2 mM MCH for 2 h at room temperature; 4) 20 μL of target DNA with varied concentrations were dropped to the modified channels, allowing for probe-target binding at 37°C for 1 h in hybridization buffer; 5) The channels were dropped with a mixed solution containing both of dATP and TdT. The TdT-mediated extension reaction was performed at 37°C in a hybridization oven (UVP, HB-1000) with constant temperature and humidity; 6) 20 μL of Ag^{+}-specific probe was added in the channels and hybridized with the extension chain to form the double-stranded (ds)DNA. Except as otherwise noted, the chip was rinsed with washing buffer and dried with a stream of nitrogen in the end of each step.

2.3. Love-SAW Measurements

The sam5 system (SAW Instruments GmbH, Bonn, Germany) was used as the Love-SAW biosensor platform. There are two types of output signal for sam5 system: phase signal and amplitude signal. The phase shift was used as output signal in our work. Measurements are performed in the two-frequency mode, a frequency difference of 0.363 (phase difference ~180^{0}) as optimized frequency value. SAW operation procedures were exactly based on the manufacturer's instructions and all experiments were performed at 25 ± 1°C. After the detection chip was prepared and the stable baseline was obtained, $AgNO_3$ and sodium borohydride solution were respectively injected at a flow rate of 40 μL/min, and an injection volume of 80 μL with 600 s total contact time was employed. The phase signal was recorded and extracted by the software after each injection. The data was directly exported to the Origin. The signals in the presence (or absence) of different concentrations of target were recorded. The mismatched DNA hybridization experiment was also conducted

View Article Online
DOI: 10.1039/C7AN00988G

by following the same procedure as mentioned above. In the practical sample assay, target DNA was spiked into human serum to obtain a certain concentration, and then the mixture was transferred to the channels of chip for hybridization.

2.4. TEM and AFM Measurements

Morphology observation of formed AgNPs in the presence and absence of target DNA was carried out via transmission electron microscopy (TEM; JEM-2100 microscope) at an acceleration voltage of 200 kv. 10 μ L of sample solution was dropped on the copper grids and air dried used for the TEM imaging. The morphology of formed AgNPs in the SAW channels was characterized with atomic force microscopic (AFM). Tapping mode image AFM was acquired under ambient conditions using a Shimadzu SPM9700 AFM system. 2 μM capture probe (20 μL), 0.5 nM target (20 μL), a 20 μL mixed solution containing both of dATP (5 mM) and TdT (0.5 U/μL), 20 μL Ag^{+}-specific probe, 10 μL $AgNO_3$ (0.5 mM) and 10 μL sodium borohydride solution (0.5 mM) were used for the formation of AgNPs.

3. Results and Discussions

3.1. Sensing Interface Architecture Design

To improve the acoustic wave response on the sensing layer surface, a synergic probe architecture that contains surface-confined prolonged DNA sequences and DNA-confined metal nanoparticles has been presented (Figure 1). Prior to introduction of target DNA that is a key to trigger subsequent template-free strand extension, the thiolated capture sequences (3'-SH) first self-assembled on gold surface of SAW sensing layer via Au-S chemistry. In the presence of target DNA, the hybridized duplex exposed with a 3'-OH terminal, serving as a specific recognition site for TdT, which can specifically catalyze the repetitive addition of dATP to elongate the target DNA and consequently produce an extended sequence with adenine(A)-rich single-stranded DNA (ssDNA). In TdT-fueled strand elongation process, dATP acts as a preferentially recognizable molecule in comparison to other mononucleotides (e.g., dTTP, dCTP, dGTP) due mainly to the 3' terminal of target DNA ended with adenine.[27,29] Thus, dATP is employed as the only recognizable molecule in TdT catalysis, aiming to obtain a controllable sequence elongation (polyA) that is beneficial to the design of Ag^{+}-specific probe. This ion-selective probe is

View Article Online
DOI: 10.1039/C7AN00988G

designed with thymine(T)-rich domain at one end, which can hybridize with the extended polyA tail, whereas the other end with cytosine(C)-rich sequence can be used to specifically bind with silver ions by forming the stable C-Ag^+-C structure.[23] This specificity has been confirmed by using our Love-SAW biosensor (Figure S1), though the Ag^+ could also stabilize other mismatches, such as C-Ag^+-A and C-Ag^+-T structures.[30] Of note, dsDNA has the higher Ag^+ incorporation efficiency than ssDNA as template.[31] It means a hybridized Ag^+-specific probe with rigid duplex structure is necessary to facilitate the trapping of more metal ions along DNA chain and improve the efficiency of in-situ synthesis of AgNPs. Upon addition of $AgNO_3$ solution, the Ag(I) ions are embedded inside the double helix of the cytosine end of Ag^+-specific probe as a stable DNA-Ag^+ complex. In the presence of $NaBH_4$, the embedded Ag^+ could be quickly reduced into clustered Ag^0 seed, namely silver nanoclusters, and grown into larger AgNPs, leading to a significant increase of phase signal. Importantly, this design involves surface-confined synergic mass effect that contributes to the enhanced acoustic wave response.

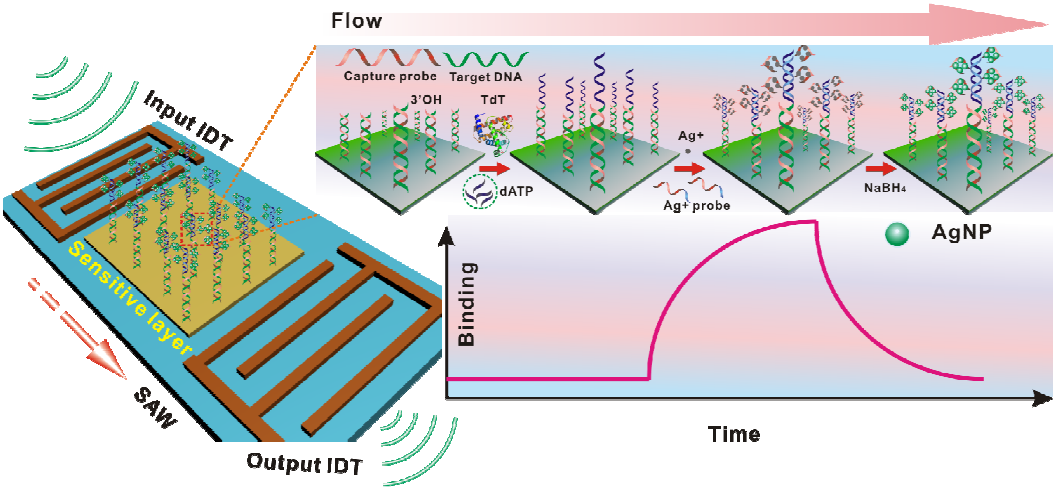

Figure 1. Schematic illustration of an SAW biosensor with an input IDT and an output IDT for highly specific and signal-amplified DNA detection by using a synergic mass effect of DNA extension and in-situ AgNPs growth.

3.2. DNA Mediated In-Situ AgNP Growth

To confirm the synthesis of AgNPs via the specific C-Ag^+-C structure, a homogeneous growth route that is identical to the in-situ surface-confined strategy was first presented via TEM analysis. As shown in Figure 2a, AgNPs with relatively uniform size were formed in a dense layout. Most of them were distributed orderly

View Article Online
DOI: 10.1039/C7AN00988G

along the "wire-like pattern" in the plane (inset in Figure 2a). In light of our previous work,[27] the length of TdT mediated homogeneous DNA elongation can reach ~500 nt (Figure S2), equal to 170 nm that is long enough to scaffold tens of nanoscale metal particles with size range centered at ~6 nm (Figure 2b). In contrast, the number of AgNPs reduced sharply in the absence of target DNA (Figure 2d). Only a few particles with diameter less than 6 nm dispersed individually (Figure 2d and 2e). This is probably due to the fact that the DNA extension reaction was inhibited without target DNA. Although the single-stranded capture probe could adsorb several silver ions by electrostatic interaction between the negatively charged DNA backbones and the positively charged Ag^{+}, the amount is limited and it is hard to form accumulated clusters.[31] Indeed, the length of capture probe (22 nt) is equivalent to 7 nm that is impossible to support a bunch of AgNPs with size ~6 nm. It means that target DNA in combination with TdT-mediated chain elongation governs the synthesis of AgNPs. AFM imaging was also used to further confirm the in-situ growth of AgNPs on DNA templates (Figure 2c and 2f). In the presence of target DNA, the AgNPs were successfully synthesized on the SAW gold chip. As demonstrated in Figure 2c, the thickness of the formed nanoparticle layer was observed to be ~23 nm (white line in Figure 2c), indicating that multiple AgNPs accumulate on the chip surface in upright or flat orientation. Nevertheless, without target DNA, the thickness of the formed

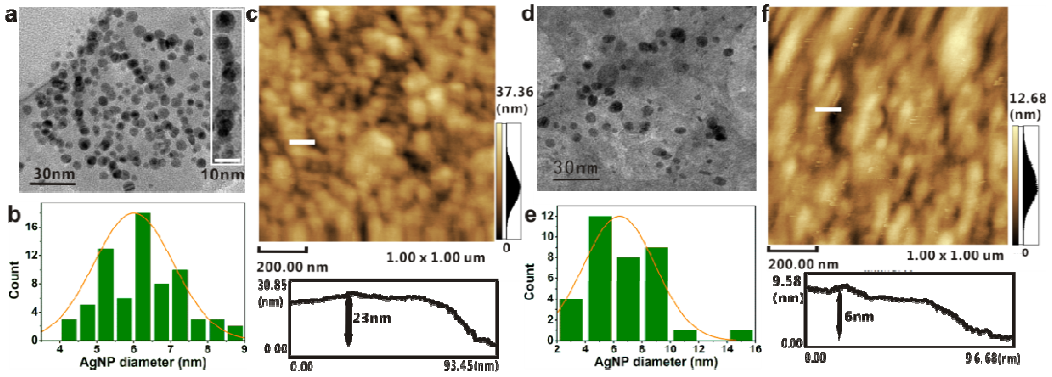

Figure 2. TEM and AFM characterization of the growth of AgNPs along with DNA strand. (a) TEM image of the synthesized AgNPs based on target DNA in combination with TdT-mediated chain elongation reaction. The inset is a magnified view of a typical 'wirelike' nanoparticle assembly in (a). (b) Particle size distribution of the synthesized AgNPs in (a). (d) TEM image of the grown silver nanoparticles in the absence of target DNA. (e) Particle size distribution of the synthesized AgNPs in (d). AFM image of the in-situ growth of AgNPs on gold surface in the presence (c) or absence of target DNA (f).The white line indicates the measured region with height showed in the bottom box.

View Article Online
DOI: 10.1039/C7AN00988G

layer was only 6 nm (white line in Figure 2f), revealing that the gold chip surface was covered with either single-layer DNA film (~7 nm capture DNA layer)or dispersed small AgNPs evolved through electrostatic adsorption on capture DNA. Both TEM and AFM results demonstrate that the TdT-mediated extension reaction in the presence of target sequence can be used to induce the formation the AgNPs on sensor surface.

3.3. Optimization of Detection Conditions

In the sensor measurement, multiple parameters, such as capture probe density, enzymatic reaction time, the concentration of $AgNO_3$ and $NaBH_4$, would impact the sensor performance by modulating both the mass and viscosity effect. Therefore, we systematically investigated these critical factors to obtain the optimal experimental conditions. The surface density of capture probe was first optimized by varying the assembly concentrations. As shown in Figure 3a, with the increase of probe concentration ranging from 0.1 to 5 μM in the presence of 0.5 nM target DNA and TdT extension system, the acoustic wave signals rose gradually and reached steady as the capture probe concentration increased to 2 μM. This trend may be attributed to the following reasons: (i) The relative high density of capture probe (2 μM) on sensing interface is able to bind more target DNA and thus provides more recognition site (3'-OH terminal) for subsequent TdT-based strand elongation as compared to that of low probe density; (ii) However, the over-dense capture probe (5 μM) on surface enables the target sequence inaccessible because of the reduced intermolecular spacing, leading to a low hybridization efficiency. Note that this signal change trend is also consistent with other sensing approaches that involve surface-confined TdT-mediated DNA extension reaction.[27, 29] Moreover, the higher concentration of capture probe can adsorb more Ag^+, which would result in high noise signal (*e.g.,* the background signal of 5 μM capture probe in Figure 3a). Therefore, the assembly concentration of capture probe was fixed at 2 μM for subsequent test (orange bar in Figure 3a).

In addition to probe density, the enzyme reaction time also controls the performance of this SAW biosensor because it governs the elongated length of polyA. We observed that the acoustic wave signal gradually increased in accompany with the proceeding of enzymatic reaction and saturated at ~1.5 h in the presence of 0.5 nM

View Article Online
DOI: 10.1039/C7AN00988G

target DNA (Figure 3b). The rapid DNA polymerization reaction at the beginning was ascribed to the sufficient substrate (dATP) for enzyme catalysis. With the depletion of dATP, the extension rate became slow. This phenomenon agrees well with another surface-confined TdT-based strand extension reaction.[33] Thus, the optimal enzymatic reaction time of 1.5 h was used to extend DNA sequence (orange bar in Figure 3b). Based on our previous report, the relative high concentration of TdT (0.5 U/μL) and dATP (5 mM) were chosen in this study because of the same gold substrate with identical probe assembly strategy.[27] Moreover, we employed excessive Ag^+-specific probe (100 μM) to complement with the extended sequence with an attempt to guarantee the polyA domain fully hybridized.

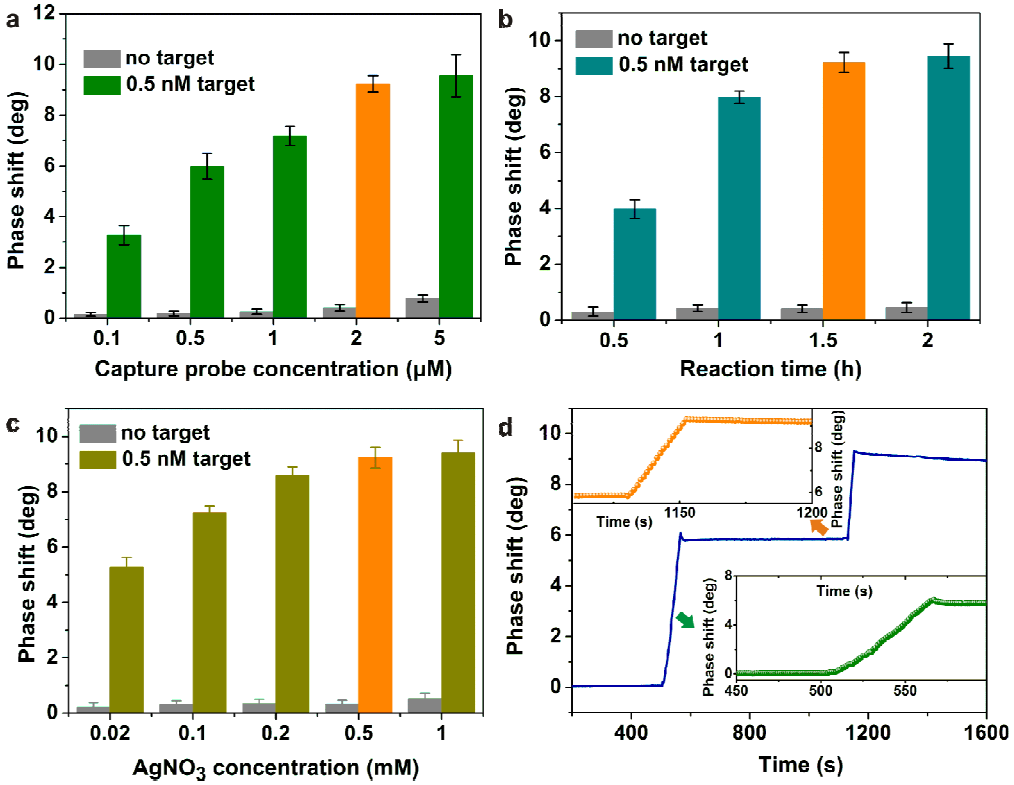

Figure 3. The influence of different parameters on the SAW sensor performance. In the presence of 0.5 nM target DNA, 0.5 U/μL TdT and 5 mM dATP, the effect of capture probe concentration (from 0.1 to 5 μM) (a), enzymatic reaction time (from 0.5 to 2 h) (b) and $AgNO_3$ concentration (from 0.02 to 1 mM) (c) on the acoustic wave signal were systematically investigated to attain the optimal parameters. The orange bars signify the optimal condition. Error bars represent standard deviations of measurements (n=3). (d) At the optimal condition with 0.5 nM target DNA, a representative dynamic phase shift response versus time for monitoring the Ag^+ binding on DNA templates (magnified in the bottom inset) and in-situ growth of AgNPs (magnified in the top inset).

View Article Online
DOI: 10.1039/C7AN00988G

Besides, the effect of $AgNO_3$ concentration on SAW sensor was also investigated. As the concentration of $AgNO_3$ increased from 0.02 mM to 0.5 mM in the presence of 0.5 nM target DNA, the phase shift enhanced by 75% and reached up to 9.23° (Figure 3c). Nevertheless, even the concentration of target DNA (~20 nt) increases as high as 1 μM, the yielded phase shift is often at the level less than 2°.[8, 16] This means the in-situ synthesis of AgNPs can significantly enhance the mass effect of SAW sensitive layer. Afterwards, the acoustic wave signal nearly reached a plateau, albeit small enhancement in signal with a further increase of $AgNO_3$ concentration (1 mM) (Figure 3c). Given the high signal-to-noise ratio, 0.5 mM $AgNO_3$ was chosen as the optimal concentration for subsequent experiments (orange bar in Figure 3c). According to previous reports, the concentration of $NaBH_4$ is often equal to that of $AgNO_3$ (1:1), thereby the optimal concentration of $NaBH_4$ is also 0.5 mM.[34, 35]

At the optimal conditions, 2 μM capture probe, 0.5 U/μL TdT, 5 mM dATP, 1.5 h enzymatic reaction time, 0.5 mM $AgNO_3$ and 0.5 mM $NaBH_4$, a real-time and dynamic Ag^+-Ag^0-AgNP transition was observed (Figure 3d). We found that the silver ions could quickly bind with the DNA structure within ~1 min (the down inset in Figure 3d). This means the change rate of phase shift (binding rate of Ag^+) is able to reach as high as 6°/min in the presence of 0.5 nM target DNA. Upon addition of $NaBH_4$, the aggregated Ag^+ reduced into Ag^0, and ultimately AgNPs, which induced a phase shift of 3° within 25 seconds, equivalent to 7.2°/min of the growth rate of AgNPs mirrored by SAW signal (the top inset in Figure 3d). It indicates that the mass effect of in-situ AgNP growth enhances 20% as compared to that of Ag^+ binding.

3.4. Sensitivity of the SAW Sensor

We next evaluated the sensitivity of this SAW sensor in DNA detection under the optimal experimental conditions by varying the concentrations of target DNA. Clearly, the phase shift enhanced dynamically along with the increase of target concentrations from 0 to 100 nM (Figure 4a). In the presence of 100 nM target DNA, the amplified SAW signal could reach up to ~27° (0-1200 s). In contrast, the same concentration of DNA sequence with the comparable length (20-22 nt) often induces very small phase shift (~1°).[16] This indicates that the TdT-mediated DNA extension in combination with in-situ AgNP growth can significantly improve the response of SAW sensor to target molecules. We observed that the signal change of acoustic wave

View Article Online
DOI: 10.1039/C7AN00988G

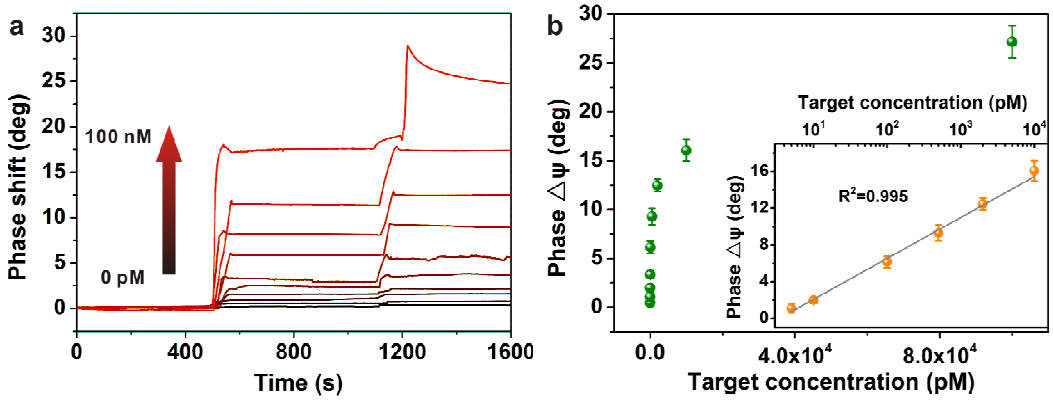

Figure 4. (a) The phase shift of the SAW sensor in response to different concentrations of target DNA: 0, 2, 5, 10, 50, 100, 500, 2000, 10000 and 100000 pM (from down to top), in combination with in-situ growth of AgNPs. (b) Target DNA concentration-dependent phase shift change corresponding to (a). Inset: the calibration curve of linear relationship between the change of phase signal (Δφ) and the logarithm of target DNA ranging from 5 pM to 10 nM. Error bars represent standard deviations of measurements (n = 3).

(Δφ: the difference value between the target-responsive phase shift and that without target) was logarithmically related to the target concentrations spanned from 5 pM to 10 nM (Figure 4b). At concentrations above 10 nM, the signal change undergoes a plateau, which is a classical saturation phenomenon of condensator charge. As shown in the inset of Figure 4b, the change of phase shift (Δφ) had a linear relationship with the logarithmic value of target DNA concentrations (C) with a regression equation

Table 2. Comparison of different assays for DNA detection.

amplification strategy	LOD	Sequence length	read-out protocol	ref
TdT/cy3-dNTP	1 pM	25 nt	fluorescence	30
TdT/biotin-dNTP/HRP	1 pM	22 nt	electrochemistry	33
avidin-AuNP/enzyme	1 fM	7229 nt	QCM	18
Quantum dots	4.21 pM	22 nt	SPR[a]	36
ligase/HRP/precipitation	1 pM	42 nt	LSAW[b]	11
graphere oxide/PCR	86.5 pM	18 nt	Love-SAW	8
TdT/AgNP	1 pM	22 nt	Love-SAW	This work

[a]SPR, surface plasmon resonance; [b]LSAW, leaky surface acoustic wave

View Article Online
DOI: 10.1039/C7AN00988G

($\Delta\varphi = 4.45\times lgC - 2.38$, $R = 0.998$), and the detection limit was estimated to be 0.8 pM (Figure S3) using $S = 3\sigma$ (S is the signal difference value of 1pM and blank, σ is standard deviation of the base line). This sensitivity is superior to the routine fluorescent and electrochemical DNA quantification methods in which they also involve the TdT extension mechanism.[29, 33] Without signal amplification, even 5 nM target DNA can only generate a phase shift less than 0.1° (Figure S4). In this case, the detection limit would be at nano-molar level that is at least 3 orders of magnitude higher than that obtained by the amplified assay (0.8 pM). To better exhibit the advantages of this synergic signal amplification strategy on SAW sensor, the associated information has been compared with other similar approaches and listed in Table 2. Of note, the sensitivity might be further improved by using either charge-neutral peptide nucleic acids as capture probe or metal deposition strategy.[14, 19]

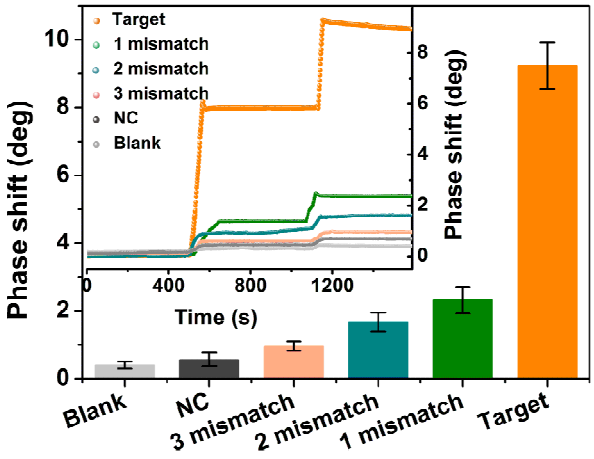

Figure 5. Selectivity of the SAW sensing interface in response to diverse DNA sequences (*i.e.,* target, 1 mismatch, 2 mismatch, 3 mismatch and non-complementary sequence), where the concentration of target DNA is 0.5 nM and the other sequences are 1 nM. Inset represents the typical phase shift of these DNA sequences including the complementary and the mismatched DNA, in conjunction with signal amplification strategy. Error bars represent standard deviations of measurements (n = 3).

3.5. Selectivity of the SAW Sensor

The selectivity of DNA biosensor is very significant, especially in single nucleotide polymorphism (SNP) assays. To evaluate the discriminating capacity of this bioassay system, we selected the perfectly complementary sequence, single-base, two-base, three-base mismatched sequences (i.e., 1 mismatch, 2 mismatch, 3 mismatch) as well as noncognate (NC) DNA sequence as targets to probe the change

View Article Online
DOI: 10.1039/C7AN00988G

of the SAW signal intensity, respectively. As shown in Figure 5, the perfectly complementary DNA demonstrated the most prominent signal change (~9.2°) even though its concentration (0.5 nM) was halved to that of mismatched sequences (1 nM). In comparison, the 1-mismatch sequence yielded only 2.3° in phase shift change, albeit slightly higher than other mismatched DNA molecules (<1.6°), which was approximately 1/4 of that of the perfectly complementary DNA (inset in Figure 5). Such ahigh selectivity might be ascribed to the unstable duplex formed by capture probe and mismatched sequences, which would denature at the reaction temperature (37°C) in TdT-mediated extension.[27, 33] As demonstrated in Figure S5, it was noticed that the free energy of secondary structure (ΔG) of target-capture duplex would increase from the initial -30.78 kcal/mol (25°C) to -22.61 kcal/mol (37°C) for 1 mismatch-capture duplex, and even up to -17.34 kcal/mol (37°C) for 2 mismatch-capture duplex. This means we can differentiate a single-base mutant sequence only at 37°C without relying on stringent thermal control by using our current SAW sensing interface and design.

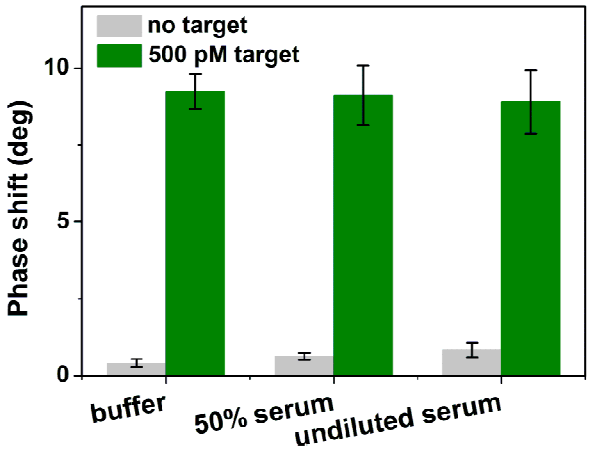

Figure 6. The SAW responses for the sensor in the detection of target DNA (0.5 nM) in buffer and complex matrices by challenging directly in undiluted and 50% human serum. Error bars represent standard deviations of measurements (n = 3).

3.6. Challenging SAW Biosensor in Complex Matrices

To further show the superiority of our SAW sensing interface, we challenged the sensor directly in clinical samples by spiking DNA targets (0.5 nM) in 50% and even undiluted (100%) human serum. As shown in Figure 6, the SAW sensor achieved a negligible variation of phase shift as incubated in different conditions including buffer, 50% human serum and undiluted human serum. It signifies that this synergic

View Article Online
DOI: 10.1039/C7AN00988G

acoustic-wave sensing interface is capable of detecting trace DNA in complex environment, though the extremely complex and multi-component nature of serum might degrade the performance of sensor. Such a superior anti-interference ability primarily benefits from the cooperative sensing interface design and the excellent base-pairing capacity of sequence specific hybridization between the capture probe and target sequence. Therefore, the developed SAW biosensing interface is promising to quantify nucleic acids in real human biofluids.

Next, the human serum was spiked with 4 different concentrations of target DNA (i.e., 0, 0.05, 0.5 and 5.0 nM) to evaluate the practicality of this SAW sensor via recovery testing. According to the linear regression equation, the corresponding concentrations of 'Found' target DNA in the human serum could be quantified. All the measurements were performed three times, and the results were summarized in Table S1. It was observed that the recoveries were all in the range of 84.0-92.0%, and the average RSD (relative standard deviation) was less than 18.2%. The results indicate that this assay works well in complex matrix, such as human serum.

4. Conclusions

In summary, we have engineered a SAW synergic mass-sensitive interface that combined template-free DNA prolongation and in-situ AgNP growth for signal-enhanced and sequence-specific DNA detection. Such a sensing interface has achieved satisfactory selectivity and improved the sensitivity of the SAW biosensor by 3 orders of magnitude (sub-picomolar level) as compared to the strategy without signal amplification. Meanwhile, this SAW sensor can readout the trace DNA target directly in the complex biofluids with ignorable interference. Besides, this strategy has several unique merits: (i) The prolonged DNA-mediated AgNPs synthesis yields an enhanced mass effect on the sensing interface; (ii) The TdT-triggered DNA extensionis template-free and highly efficient; (iii) This synergic sensing interface design is also amenable to tailor-engineer other signal-amplification detection modes, particularly those relied on gold surface.[37-40] By integrating this synergic mass-sensitive SAW sensing interface with microfluidics may further boost its advantages, such as multiplexing assay and single-step readout, for potential on-site clinical diagnostics.[41, 42]

View Article Online
DOI: 10.1039/C7AN00988G

Conflicts of interest

The authors declare no competing financial interest.

Acknowledgments

This work was supported by the National Natural Science Foundation of China (Grant No. 21305034, 21475034 and 21675041) and Hubei Province health and family planning scientific research project (Grant No. WJ2017Q032). Dr. Yulin Zhang thanks the support of Natural Science Fund of Hubei Province (2016CFB220)

Supporting Information

SAW signal of 5 nM target DNA without signal amplification, free energy of secondary structure of the mismatch-target duplex by NUPACK analysis and Table for recovery testing. This material is available free of charge via the Internet at http://pubs.rsc.org.

References

1. K. Länge, B. E. Rapp and M. Rapp, *Anal. Bioanal. Chem.*, 2008, **391**, 1509-1519.
2. A. Afzal, N. Iqbal, A. Mujahid and R. Schirhagl, *Anal. Chim. Acta.*, 2013, **787**, 36-49.
3. G. Papadakis, J. Friedt, M. Eck, D. Rabus, G. Jobst and E. Gizeli, *Biomed. Microdevices.*, 2017, **19**, 16.
4. L. A. Francis, J.-M. Friedt, C. Zhou and P. Bertrand, *Anal. Chem.*, 2006, **78**, 4200-4209.
5. D. H. Dinh, É. Pascal, L. Vellutini, B. Bennetau, D. Rebière, C. Dejous, D. Moynet, C. Belin and J.-P. Pillot, *Sens. Actuators, B*, 2010, **146**, 289-296.
6. A. G. Ayankojo, A. Tretjakov, J. Reut, R. Boroznjak, A. Öpik, J. Rappich, A. Furchner, K. Hinrichs and V. Syritski, *Anal. Chem.*, 2016, **88**, 1476-1484.
7. A. Tretjakov, V. Syritski, J. Reut, R. Boroznjak and A. Öpik, *Anal. Chim. Acta.*, 2016, **902**, 182-188.
8. X. Liu, J.-Y. Wang, X.-B. Mao, Y. Ning and G.-J. Zhang, *Anal. Chem.*, 2015, **87**, 9352-9359.

View Article Online
DOI: 10.1039/C7AN00988G

9. N. Fourati, M. Seydou, C. Zerrouki, A. Singh, S. Samanta, F. Maurel, D. K. Aswal and M. Chehimi, *ACS Appl. Mater. Interfaces*, 2014, **6**, 22378-22386.
10. F. J. Gruhl and K. Länge, *Analyt. Biochem.*, 2012, **420**, 188-190.
11. Q. Xu, K. Chang, W. Lu, W. Chen, Y. Ding, S. Jia, K. Zhang, F. Li, J. Shi, L. Cao, S. Deng and M. Chen, *Biosens. Bioelectron.*, 2012, **33**, 274-278.
12. S. M. Balashov, O. V. Balachova, A. V. U. Braga, A. P. Filho and S. Moshkalev, *Sens. Actuators, B*, 2015, **217**, 88-91.
13. M. Asad and M. H. Sheikhi, *Sens. Actuators, B*, 2014, **198**, 134-141.
14. J. Lee, Y.-S. Choi, Y. Lee, H. J. Lee, J. N. Lee, S. K. Kim, K. Y. Han, E. C. Cho, J. C. Park and S. S. Lee, *Anal. Chem.*, 2011, **83**, 8629-8635.
15. X. Zhang, Y. Zou, C. An, K. Ying, X. Chen and P. Wang, *Sens. Actuators, B*, 2015, **217**, 100-106.
16. T. M. A. Gronewold, A. Baumgartner, E. Quandt and M. Famulok, *Anal. Chem.*, 2006, **78**, 4865-4871.
17. F. Höök, A. Ray, B. Nordén and B. Kasemo, *Langmuir*, 2001, **17**, 8305-8312.
18. Y. Weizmann, F. Patolsky and I. Willner, *Analyst*, 2001, **126**, 1502-1504.
19. F. Gao, J. Lei and H. Ju, *Anal. Chem.*, 2013, **85**, 11788-11793.
20. X. Tian, X.-J. Kong, Z.-M. Zhu, T.-T. Chen and X. Chu, *Talanta*, 2015, **131**, 116-120.
21. H.-C. Yeh, J. Sharma, J. J. Han, J. S. Martinez and J. H. Werner, *Nano Lett.*, 2010, **10**, 3106-3110.
22. H. Xu and K. S. Suslick, *Adv. Mater.*, 2010, **22**, 1078-1082.
23. I. Diez and R. H. A. Ras, *Nanoscale*, 2011, **3**, 1963-1970.
24. Y. Yuan, W. Li, Z. Liu, Z. Nie, Y. Huang and S. Yao, *Biosens. Bioelectron.*, 2014, **61**, 321-327.
25. X. Liu, R. Hu, Z. Gao and N. Shao, *Langmuir*, 2015, **31**, 5859-5867.
26. J.-L. Ma, B.-C. Yin, H.-N. Le and B.-C. Ye, *ACS Appl. Mater. Interfaces*, 2015, **7**, 12856-12863.
27. F. Yang, X. Yang, Y. Wang, Y. Qin, X. Liu, X. Yan, K. Zou, Y. Ning and G.-J. Zhang, *Anal. Chem.*, 2014, **86**, 11905-11912.
28. Q. Shen, L. Han, G. Fan, J.-R. Zhang, L. Jiang and J.-J. Zhu, *Anal. Chem.*, 2015, **87**, 4949-4956.

View Article Online
DOI: 10.1039/C7AN00988G

29. Y. Wan, P. Wang, Y. Su, L. Wang, D. Pan, A. Aldalbahi, S. Yang and X. Zuo, *ACS Appl. Mater. Interfaces*, 2015, **7**, 25618-25623.

30. V. Tjong, H. Yu, A. Hucknall, S. Rangarajan and A. Chilkoti, *Anal. Chem.*, 2011, **83**, 5153-5159.

31. D. Majumdar, A. Singha, P. K. Mondal and S. Kundu, *ACS Appl. Mater. Interfaces*, 2013, **5**, 7798-7807.

32. C. Russell, S. Roy, S. Ganguly, X. Qian, M. H. Caruthers and M. Nilsson, *Anal. Chem.*, 2015, **87**, 6660-6666.

33. Y. Wan, H. Xu, Y. Su, X. Zhu, S. Song and C. Fan, *Biosens. Bioelectron.*, 2013, **41**, 526-531.

34. J.-J. Liu, X.-R. Song, Y.-W. Wang, A.-X. Zheng, G.-N. Chen and H.-H. Yang, *Anal. Chim. Acta.*, 2012, **749**, 70-74.

35. J. T. Petty, J. Zheng, N. V. Hud and R. M. Dickson, *J. Am. Chem. Soc.*, 2004, **126**, 5207-5212.

36. A. S. Ghrera, M. K. Pandey and B. D. Malhotra, *Biosens. Bioelectron.*, 2016, **80**, 477-482.

37. J. Zhang, S. Song, L. Wang, D. Pan and C. Fan, *Nat. Protoc.*, 2007, **2**, 2888-2895.

38. H. Pei, N. Lu, Y. Wen, S. Song, Y. Liu, H. Yan and C. Fan, *Adv. Mater.*, 2010, **22**, 4754-4758.

39. M. Lin, J. Wang, G. Zhou, J. Wang, N. Wu, J. Lu, J. Gao, X. Chen, J. Shi, X. Zuo and C. Fan, *Angew. Chem. Int. Ed.*, 2015, **54**, 2151-2155.

40. M. Lin, P. Song, G. Zhou, X. Zuo, A. Aldalbahi, X. Lou, J. Shi and C. Fan, *Nat. Protoc.*, 2016, **11**, 1244-1263.

41. F. Yang, X. Zuo, Z. Li, W. Deng, J. Shi, G. Zhang, Q. Huang, S. Song and C. Fan, *Adv. Mater.*, 2014, **26**, 4671-4676.

42. S. Li, Y. Wan, Y. Su, C. Fan and V. R. Bhethanabotla, *Biosens. Bioelectron.*, 2017, **95**, 48-54.

View Article Online
DOI: 10.1039/C7AN00988G

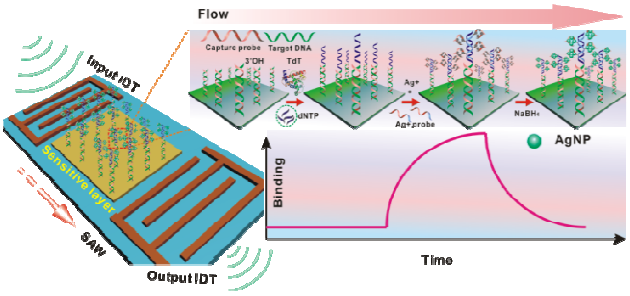

SAW biosensor harmonizes the surface mass effect for signal-amplified and sequence-specific DNA detection in blood serum.